Ductile fracture nucleation ahead of sharp cracks

DONATO FIRRAO, Dipartimento di Scienza dei Materiali e Ingegneria Chimica, Politecnico di Torino, Turin, Italy
ROBERTO ROBERTI, Dipartimento di Chimica-Fisica Applicata, Politecnico di Milano, Milan, Italy

Abstract
Models proposed up to now to describe ductile fracture nucleation ahead of sharp cracks are reviewed and mathematical relationships, derived for calculating fracture toughness, discussed. A new model, based on the phenomenon of crack tip blunting, has been conceived. Equations relating J_{Ic} or K_{Ic} to inclusion spacing in a metal alloy, to its strain-hardening properties and to the maximum strain acting at ductile fracture nucleation in a blunt notch specimen have been derived. Their validity is proved with experimental results on a number of low C steels.

Riassunto
Si sono esaminati i modelli finora proposti per descrivere il fenomeno della nucleazione di fratture duttili a partire da cricche con raggio di fondo infinitesimo e si sono discusse le relazioni matematiche derivate da tali modelli per il calcolo della tenacità a frattura. È stato introdotto un nuovo modello che tiene conto del fenomeno dell'aumento del raggio di fondo di una cricca prima che da questa si origini una rottura. Sono state inoltre derivate equazioni che permettono di calcolare i valori di J_{Ic} o K_{Ic} per una lega metallica, partendo dalla spaziatura media delle inclusioni non metalliche, dalle caratteristiche di incrudimento della lega e dall'allungamento massimo agente alla radice di un intaglio non acuto nel momento della nucleazione della frattura duttile. I risultati sperimetali ottenuti con parecchi acciai a basso tenore di carbonio hanno consentito di confermare la validità del modello e delle relazioni proposte.

Introduction

For a full understanding of the process that leads to fully ductile fracture initiation and propagation in the triaxial stress field ahead of a sharp crack, you have to model completely the complex interplay between the metal matrix flow characteristics and the microstructural features that can act as substrates for void formation at various levels of stress.
The numerous attempts of this kind conducted over the past 20 years have aimed at establishing a link between readily obtainable mechanical properties, as provided by a simple tension test, and some kind of microstructural parameter on one side and the fracture toughness of a material (K_{Ic} or J_{Ic}) on the other, in order to avoid the lengthy tests necessary to establish these parameters, and eventually speed up material control procedures.
A secondary more ambitious goal has been to provide the metallurgical engineer with a tool for designing tougher and more reliable alloys for structural needs.
A review of plane strain ductile fracture models is presented here, followed by a new proposal, with the experimental data supporting the mathematical relationships derived from it.

Proposed Ductile Fracture Nucleation Models

A fracture criterion adopted in many theories is that of Rice and Johnson (1); they stated that the onset of crack propagation occurs when a critical strain is reached over a definite distance from the crack tip, which is of the same order of magnitude as the critical crack-tip opening displacement (COD).
The critical COD in plane strain, δ_{Ic}, is in turn a function of the fracture toughness, K_{Ic}, via the usual correlation

$$\delta_{Ic} = m\, K_{Ic}^2/E\sigma_y \qquad (1)$$

where E is the Young's modulus, σ_y the yield strength and "m" a numerical constant varying between 0.425 and 0.717, according to various authors.
The above distance is a function of the microstructure of the material, i.e. of a microstructural *characteristic* distance (2). The concept had already been laid down in Krafft's (3) earlier model,which assumed the existence of a small "process" zone ahead of the crack tip. Zone elements were idealized as circular tensile ligaments, clinching the throat of the crack until they are drawn out to the point of tensile instability, where their rupture became inevitable. Consequently, Krafft proposed the following equation relating the plane strain fracture toughness, K_{Ic}, to material parameters

$$K_{Ic} = EN\sqrt{(2\pi d_T)} = E\,\varepsilon_i\sqrt{(2\pi d_T)} \qquad (2)$$

E is the Young's modulus, N is the strain-hardening exponent (equal to the uniform elongation strain at the instability of a tensile specimen, ε_i), and d_T is the diameter of the idealized tensile specimens. d_T should be set equal to the average inclusion spacing in the matrix, *s*, as also later demostrated by Birkle, Wei, and Pellissier (4).
The model also works with a reasonably good approximation when fracture surfaces show a series of

parallel ridges and troughs at constant spacing, as in precipitation hardening stainelss steel (5) or maraging steel (6). In the latter case, a close correlation was observed between experimental values of K_{Ic} and the ones computed introducing in Eq. 1 the ridge-to-ridge distance in place of d_T.
Later models emphasized that the fracture toughness of a material should be more strongly dependent on the plane strain ductility $\varepsilon_{f,ps}$ (7) than the axisymmetric ductility, since the former reflects more closely the stress state conditions at the crack tip.
In this sense, Krafft (8) had already modified his original model proposing that

$$K_{Ic} = E\,[(\sigma_y + \sigma_{uts})/E + N/2]\,\sqrt{(2\pi\, d_T)} \qquad (3)$$

where σ_y and σ_{uts} are the yield and tensile strengths of the material.
Hahn and Rosenfield (9) suggested that $\varepsilon_{f,ps}$ could be obtained from the true fracture strain in uniaxial tension, ε_f, setting $\varepsilon_{f,ps} = \varepsilon_f/3$.
Hypothesizing a relationship between the critical COD, the critical maximum strain at the crack tip, and the width of the plastic zone, which is a function of the square of the strain-hardening coefficient of the material, they proposed the semi-empirical equation,

$$K_{Ic} = N\sqrt{\left(\frac{2}{3}E\sigma_y\varepsilon_f \cdot 0.0254\right)}\ (MN\cdot m^{-3/2}) \qquad (4)$$

which is to be replaced by the following relation in the case of materials with an unusually low strain-hardening exponent ($N<0.02$)

$$K_{Ic} = 5\sqrt{\left(\frac{2}{3}E\sigma_y\varepsilon_f\,(N^2+0.0005)\,10^{-3}\right)}\ (MN\cdot m^{-3/2}) \qquad (5)$$

The relationship was found valid by Slatcher and Knott (10) in low alloy - high strength steels quenched and tempered at 500 – 600 °C, but not verified when the same steels are tempered at lower temperatures.
The same argument was used by Chen and Knott (11) to derive the following relationship for calculating the value of K at fracture initiation (K_i);

$$K_i = \sqrt{\left(\frac{b}{m\cdot 10A}\,E\,\sigma_c\,\sigma_y\,N^2\,s\,D^{-1}\right)} \qquad (6)$$

where b is the Burgers vector, A is a factor of proportionality having a magnitude of the order of $Gb/2\pi$ (G is the shear modulus) and σ_c is the cohesion strength at the matrix-particle interface. D is the diameter of the inclusion.
To emphasize the role of the second-phase particles on fracture toughness Hahn and Rosenfield (12) proposed different equations

$$K_{Ic} = \sqrt{\left(2\sigma_y E s\right)} \qquad (7)$$

$$K_{Ic} = \left\{2\sigma_y \cdot E\left(\frac{\pi}{6}\right)^{1/3}\cdot D\right\}^{1/2}\cdot v^{-1/6} \qquad (8)$$

Eqs. 7 and 8 reflect a model involving fracture of (or decohesion at) large second-phase particles (D is the diameter of cracked particles) and the subsequent linking of associated expanded voids by rupture of the intervening ligament, as set by the approximate failure criterion proposed by Rice and Johnson (1); i.e. a crack propagates when the extent, *x*, of the heavily deformed region ahead of the crack is comparable to the average width of the umbroken ligaments (*s*). Eq. 8 is derived in consideration of the fact that the volume fraction of a dispersed phase (*v*) is proportional to the cube of the *D*/*s* ratio.
Broek (13) had already pointed out that both second-phase volume fraction and particle spacing control the fracture toughness of a given material, implying that the critical crack tip fracture strain, ε_t, is a function of the volume fraction. He derived

$$K_{Ic} = \frac{E}{1+\nu}\,(2\pi s)^{1/2} f(1/v) \qquad (9)$$

where ν is the Poisson's ratio.
Experimental independent determinations of K_{Ic} from 3-point bend test specimens, and of $\varepsilon_{f'ps}$ on Clausing's bars for 4 steels, led Barsom and Pellegrino (14) to the following semiempirical correlation between the two quantities

$$K_{Ic} = A\,\varepsilon_{f,ps}^{h}\sqrt{\sigma_y} \qquad (10)$$

with h being very close to 2 for low carbon alloy steels and to 3 for 18 pct Ni (grade 250) maraging steel. A is a set constant for a given steel to be determined in each case. Infact, the model implies a proportionality between the critical crack tip strain supposed equal to $\varepsilon_{f,ps}$ and δ_{Ic};

$$\varepsilon_f = \beta\,\delta_{Ic}^{1/2h}$$

since m in Eq. 1 is set equal to 1, A in Eq. 10 is equal to $\sqrt{E/\beta^{2h}}$.

An experimental correlation between ε_t and δ_i, the COD at crack propagation, is according to Smith and Knott (15): $\delta_i = \varepsilon_t \cdot l$ where l can be considered as the gage length along the crack contour or notch tip contour over which the strain can be considered approximately constant; $l = \varrho$ or $l = 1.2\varrho$ in the case of a blunt notch with end radius egual to ϱ (Griffiths and Owen, (16)).
For sharp cracks in mild steels l has to be set equal to the inclusion spacing, *s* (Chipperfield and Knott, (17)), so that the following equations can be derived upon conservatively setting δ_{Ic} equal to δ_i:

$$K_{Ic} \approx \sqrt{(2\sigma_y E \cdot \varepsilon_t \cdot s)} = \sqrt{(2\sigma_y \cdot E \cdot \varepsilon_{f,ps} \cdot s)} \qquad (11)$$

which can be approximated as,

$$K_{Ic} \approx \sqrt{\left(\frac{2}{3}\sigma_y \cdot E \cdot \varepsilon_f \cdot s\right)} \qquad (11')$$

Other models make a linkage between the plastic zone and the applied stress intensity factor.
Schwalbe (18, 19) hypothesizes a strain distribution within the plastic zone, analogous to the one proposed by Rice (20) for shear strain upon Mode III loading; then by setting again that the plane strain fracture strain has to be reached over a distance equal to the interparticle spacing, he proposes

$$K_{Ic} = \frac{\sigma_y}{1-2\nu}\sqrt{\left(s\pi\,(1+N)\left[\frac{\varepsilon_{f,ps}}{\sigma_y} \cdot E\right]^{1+N}\right)} \qquad (12)$$

or

$$K_{Ic} = \frac{\sigma_y}{1-2\nu}\sqrt{\left(s\pi\,(1+N)\left[\frac{\varepsilon_{f,ps}}{\sigma_y} \cdot E \cdot \frac{N}{1+N}\right]^{1+N}\right)} \qquad (13)$$

Alternatively Osborne and Embury (21) considered the work done along the x - axis, in the region between *s* and the elastic-plastic boundary, equal to G_{Ic}. They assumed a strain distribution within the plastic zone of the type proposed by Rice and Rosengren (22) and a critical strain (this time equal to $\frac{2}{3}\varepsilon_f$) again reached over a distance equal to *s* from the crack tip. Their formulation, valid for materials with $\sigma_y \approx 700$MPa, reads

$$K_{Ic} = \sqrt{\left(\frac{2}{3}\sigma_{uts} \cdot E \cdot \varepsilon_f \cdot s \cdot \ln\frac{2}{3}\frac{\varepsilon_f}{\varepsilon_y}\right)} \qquad (14)$$

The crack tip blunts before fracture is nucleated in quasi-static loading. The phenomenon is taken into account in the formulation of further models. They consider numerical solutions for the strain distribution in front of the blunted tip, adopted following Rice and Johnson's (1) calculations for a rigid ideal plastic material.
With this approach, assuming again that at fracture the critical strain has to be reached over a distance from the crack tip equal to the interparticle spacing, Schwalbe (19) set

$$\varepsilon_{f,ps} = \frac{0.44\,\delta_{Ic}}{s} - 0.23$$

and assuming m (Eq. 1) = 0.5 obtained

$$K_{Ic} = \sqrt{[(4.55\,\varepsilon_{f,ps} + 0.23)\,E\,\sigma_y s]} \qquad (15)$$

Similarly Pandey and Banerjee (23) set

$$\varepsilon_{f,ps} = f\frac{\delta_{Ic}}{x_f}$$

with x_f being the extent of the zone over which the critical strain is to be reached at fracture and f a numerical constant.
Then

$$K_{Ic} = \sqrt{\left(\frac{\varepsilon_{f,ps} \cdot x_f \cdot E \cdot \sigma_y}{m \cdot f}\right)} \qquad (16)$$

Ritchie, Server, and Wullaert (24) equalled x_f to a microstrutturally significant characteristic distance l_o and set m = 0.6 following the McMeeking (25) small scale yielding formulation. To single out the precise value of $\varepsilon_{f,ps}$ to be inserted into Eq. 16, they tested a series of circumferential notch tensile specimens with varying values of ϱ, the notch-end radius, in order to determine the variation of the fracture strain as a function of the stress state (Mackenzie, Hancock, and Brown, (26)). Then, after identifying the particular stress state acting at the appropriate l_o distance from the crack-tip, employing a numerical solution by Rice and Johnson (1), the right value of $\varepsilon_{f,ps}$ valid for each steel can be determined. Experiments on SA533B and SA302B steels showed that the best values of l_o were in the region of 6-7 times the interparticle spacing for the former, and about equal to *s* for the latter.

Critical Analysis of Proposed Models

Analyzing the above listed equations, it can be seen that K_{Ic} has been consistently linked to 4 tensile quantities (σ_y, E, N, and some type of fracture or instability strain) and to a microstructural parameter, *s*. As regarding the four mechanical characteristics, E does appear in all the relationships, whereas σ_y is

missing only in Eq. 2. Eq. 4 does not show either N or any type of strain (the 2 quantities can be somehow related); N is also absent in Eqs. 7, 8, 9, 10, 11, 11'. The only relationship in which neither *s* nor any other microcstructural parameter appear is Eq. 10, although an indirect linkage between K_{Ic} and the microstructure can also be found there; in fact, σ_y has been related to *s* (27, 28), whereas ε_f or N have been related to the second-phase volume fraction (see Hahn and Rosenfield (12) and Pickering (29) for reviews). The latter can explain why *v* appears alongside *s* only in Eq. 9.

All the 5 tensile and microstructural quantities appear simultaneously only in Eqs. 12 and 13.

Eqs. 2, 3, 4, 7, 11, 12, 13, 14, 15 can be readily employed to calculate K_{Ic} via the 5 above listed quantities. Calculations reported by Schwalbe (19) and others, based on the data listed by him, show that the agreement between experimental and computed values of fracture toughness can be considered only fair in the best cases and decidedly bad in the others.

Obviously, the quantities whose values are most affected by error are *s* and the value to be inserted in place of the crack tip strain. Regarding the former, the uncertainty arises from the phenomenological observation that not all second-phase particles within a material have associated voids at the same level of stress. It is generally accepted (12) that larger particles crack or decohere at lower levels of stress or strain than intermediate or fine ones. Void formation with large inclusions is enhanced by the triaxial state of stress that develops in plane strain conditions in the vicinity of the stress concentration. Then, the critical stages in fracture initiation when loading a precracked specimen are (i) the linkage of the crack-tip with some closely located voids at different positions along the crack front and (ii), most of all, the linkage of the crack front protrusions generated in the above way. These coalescence processes are the ones that control the real critical crack-tip growth and conversely COD at initiation.

Under the above assumptions, resistance to the onset of crack growth, once voids are generated, is controlled by the capacity of the matrix material between voids associated with large particles to further straining under increasing stress. Such a resistance is enhanced by the ability of the material to strain-harden and is foreshortened by the tendency to strain localization in narrow slip bands, i.e. to shearing instability. These characteristics are not independent of one another (30): materials with higher N values show a greater resistance to the development of shearing instabilities than those with lower associated N values.

The matrix material between voids comprises intermediate and fine particles which favour strain localization and therefore tend to limit fracture deformation (12). Consequently, their role can be stated as largely detrimental to fracture toughness.

From what precedes, it can be inferred that the *s* value which controls fracture toughness is the one related to the spacing of large inclusions, especially in mild alloys where large plastic zones develop at the crack-tip. Instead, the volume fraction of all the inclusions, large, intermediate, and fine, determines the maximum strain that can be sustained in the region close to the crack-tip before the onset of critical growth. Besides the inclusion volume fraction, the stress state acting at the crack-tip at the moment of fracture nucleation also controls such a limiting strain (24).

For such a reason the suggestion by Hahn and Rosenfield or Osborne and Embury (21) that the strain to be taken into account is some fraction of the uniaxial fracture strain, can be considered as leading to an only a rough approximation. Better attempts to reproduce the stress state at a stress concentration are those made by the use of Clausing's bars (2, 19).

It has to be noted that, with the former method, it is possible to reproduce the plane strain situation acting at the stress concentration without indeed copying the same small gage length or steep stress gradients. In fact, results in predicting experimental K_{Ic} values have met with limited success.

The best procedure envisioned up to now, to identify the strain acting at the crack tip at the moment of fracture nucleation, is the one proposed by Ritchie and colleagues (24) by the use of circumferentially notched specimens as outlined previously. Unfortunately, it is a lengthy one and, furthermore, the results reported by the authors indicate that a precise prediction of K_{Ic} is not always possible, owing to the lack of a clear-cut relationship between l_o and the interparticle spacing valid for all metal alloys.

A new model for ductile fracture nucleation

The researches performed in recent years on cracked specimens to obtain accurate variations of applied J-integral values as a function of crack extension (J R-curves) have demostrated that the early stages of crack growth stem from the blunting of the crack under increasing loads. The passage from vanishing crack tips to finite root notches terminates when the root radius (ϱ) reaches a definite value (ϱ_{eff}). The existence of such a limiting radius in plane strain ductile fracture has been proved by Chipperfield and Knott (17) on a 0.17% C,

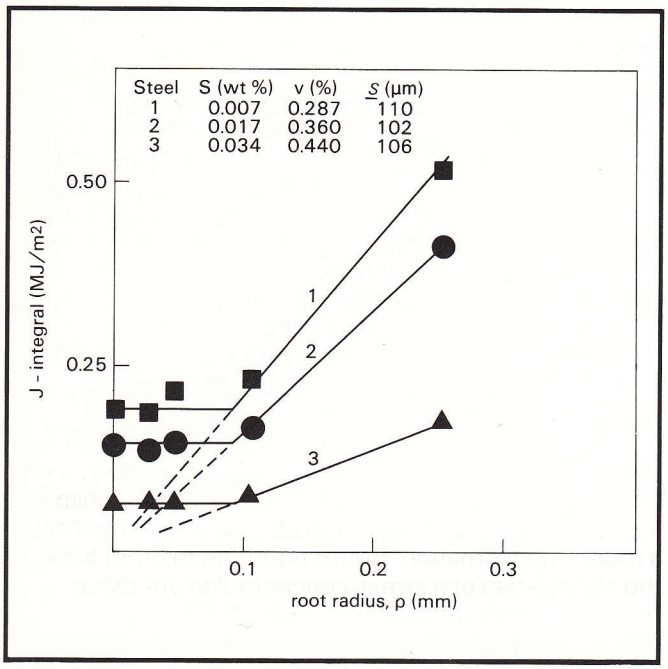

Fig. 1 - Applied J-integral values at fracture initiation vs. the notch root radius of 3-point bend specimens fabricated with C-Mn steels with various sulfur and inclusion contents (v) and similar inclusion spacing (s). Cracks and notches were in the T-L direction.

1.95% Mn steel and a high strength Ni-Cr-Mo-V steel, by Lereim and Embury (31) on a variety of HSLA steels and on AISI 4340 steel, and more recently by Roberti and colleagues (32) on different types of 0.17% C, 1.33% Mn steels (Fig. 1). All the above authors have reported that fracture toughness results from notched specimens with ϱ smaller than ϱ_{eff} were identical to those obtained employing precracked specimens. It can also be seen that, prior to fracture advance, both types of specimens originate analogous "stretch zones" (Fig. 2). It can be inferred that both types of specimens fail by the same mechanism, i.e. they all develop a blunt notch with $\varrho = \varrho_{eff}$ and afterwards fracture when the maximum strain at the notch tip reaches a limiting value.

Furthermore, it has been demonstrated that blunt notch specimens of a given material with $\varrho \geq \varrho_{eff}$ reach a ductile fracture initiation stage because a constant limiting strain $\varepsilon_{max,f}$ is achieved at the notch root. In fact, Firrao and colleagues (33, 34, 35), Roberti and co-workers (32) demonstrated that applied J-integrals at the onset of fracture vary linearly with ϱ (see Fig. 1), thus proving the validity of a ductile fracture initiation model from blunt notches originally proposed by Begley, Logsdon, and Landes (36). The model took into account the equation derived by Rice (37) to relate the applied J-integral, the notch-end radius, and the strain-hardening properties of a material to the maximum strain acting at the notch root, ε^*_{max};

$$\varepsilon^*_{max} = \varepsilon_y \left[\frac{(N+1/2)\,(N+3/2)\,\Gamma\,(N+1/2)}{\Gamma\,(1/2)\,\Gamma\,(N+1)} \; \frac{J}{\sigma_y \varepsilon_y \varrho} \right]^{\frac{1}{1+N}} \quad (17)$$

where Γ is the mathematical gamma function. Eq. 17 tells that, if a critical notch root strain, $\varepsilon^*_{max,f}$, is the appropriate parameter for ductile crack initiation at the root of the notch, a plot of the applied J values at the onset of crack growth versus ϱ should indeed be a straight line passing through the origin.

Upon setting,

Fig. 2 - Stretch zones developing at the root of a fatigue crack (a) or of a 0.03 mm radius notch (b) in steel 1 specimens loaded up to a fracture..

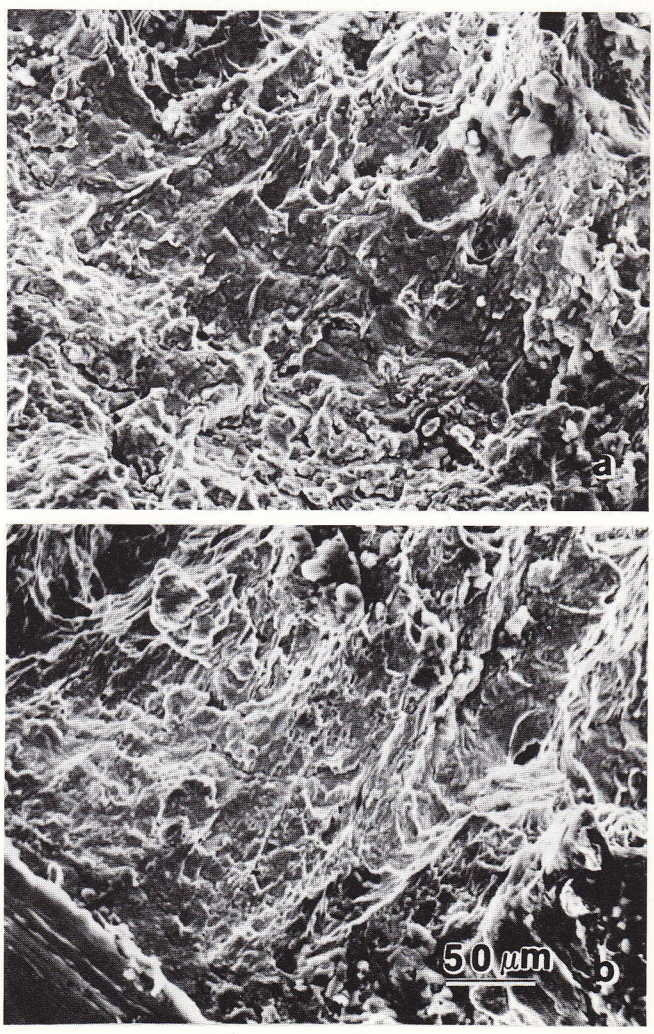

$$F(\Gamma(N)) = \frac{(N+1/2)\,(N+3/2)\,\Gamma(N+1/2)}{\Gamma(1/2)\,\Gamma(N+1)}$$

Eq. 17 can then be written in the following form (38),

$$J_A = \sigma_y^{(1-N)} \frac{\varepsilon^{*(N+1)}_{max,f} E^N}{F(\Gamma(N))} \varrho_{eff} \qquad (18)$$

where J_A is the J-integral applied at fracture initiation in a notched specimen with notch root radius $\varrho \geq \varrho_{eff}$. Eq. 18 either adequately describes the resistance of blunt notch specimens to ductile rupture nucleation or can be employed to calculate an accurate value of the maximum strain active at a notch root before the onset of crack growth. For instance, values of $\varepsilon^*_{max,f}$ equal to 0.991, 0.876, and 0.474 have been obtained for steels 1, 2, and 3 of Fig. 1 (39).

From what precedes it is clear that the new model proposed for ductile fractures originating from a sharp crack, based on the hypothesis of tip blunting up to a limiting radius (ϱ_{eff}), allows to calculate the crack-tip strain at onset of fracture from results obtained with blunt notch specimens. Thus, the following formula can be written to compute the fracture toughness J_{Ic},

$$J_{Ic} = \sigma_y^{(1-N)} \frac{\varepsilon^{*(N+1)}_{max,f} E^N}{F(\Gamma(N))} \varrho_{eff} \qquad (19)$$

By dividing Eq. 18 by Eq. 19 one obtains,

$$\frac{J_A}{J_{Ic}} = \frac{\varrho}{\varrho_{eff}} \qquad (20)$$

The experiments carried out by the authors on C-Mn steels with different microstructures (Fig. 1) allow us to prove that ϱ_{eff} is of the same order as s, which is to be taken as the spacing between major inclusions in accordance with previous considerations.

Therefore, it is possible to write,

$$\frac{J_A}{J_{Ic}} = \frac{\varrho}{s} \qquad (21)$$

Fig. 3 reports plots of J_A/J_{Ic} vs. ϱ/s for the steels of Fig. 1. For values of $\varrho/s \geq 1$ the interpolating line of all the results has a 45° slope as predicted by Eq. 21 and levels off horizontally when the root radius falls below the interparticle spacing.

Similar results had also been obtained by Chipperfield and Knott (17) who measured δ_{Ic} values and COD at fracture initiation from notches (δ_A) on a number of low C steels with different Mn contents. The resulting plot is presented in Fig. 4, where l has been set by the

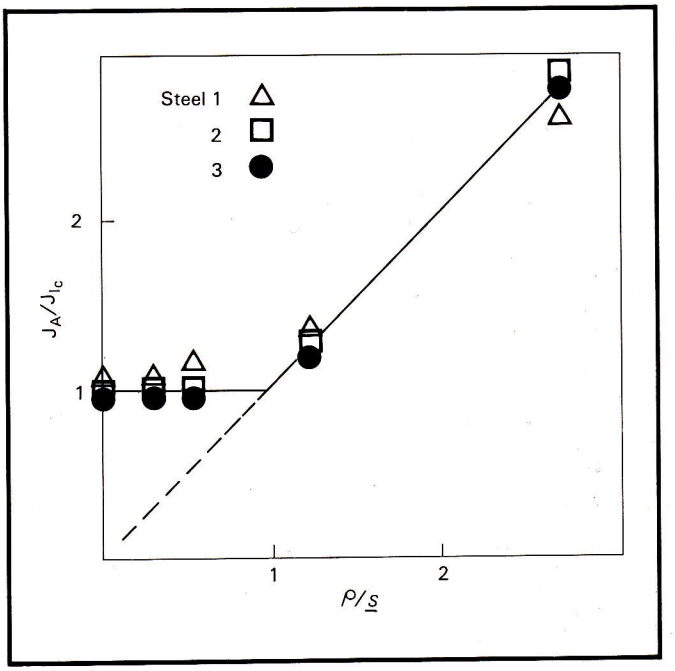

Fig. 3 - Fracture toughness results of Fig. 1 presented as adimensioned plots of the J_A/J_{Ic} ratio vs. ϱ/s (see Eq. 21).

Fig. 4 - Fracture toughness results by Chipperfield and Knott (17) on a series of C-Mn steels (see Table 1). Data are presented as in Fig. 3; l = 1.1 ϱ. Steel T has been tested with the stress concentration in 3 different orientations with respect to the rolling direction.

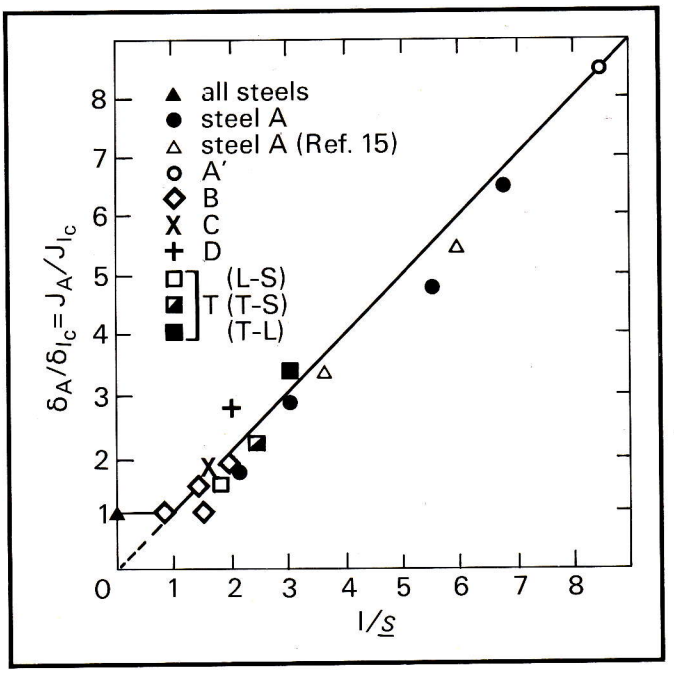

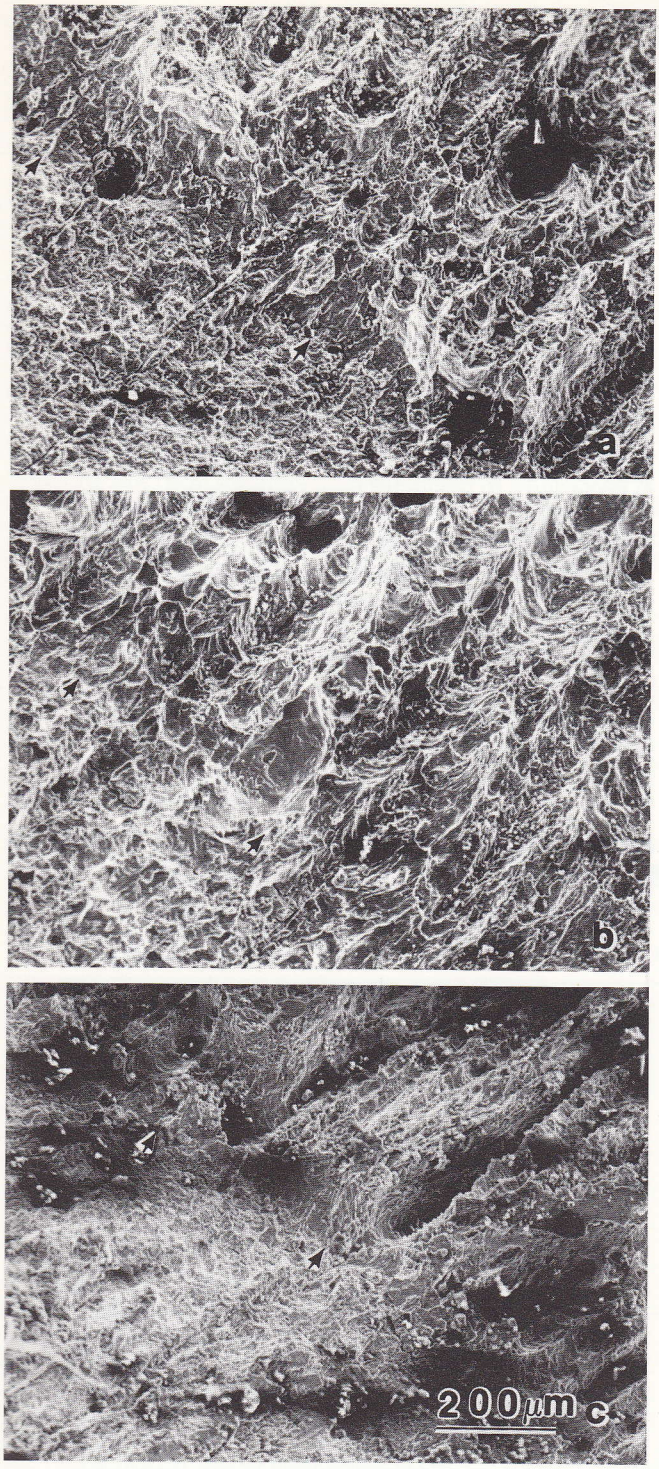

Fig. 5 - Fracture surfaces of precracked specimens of steels 1 (a), 2 (b), and 3 (c) of Fig. 1. Arrows indicate the end of the fatigue pre-cracks.

authors as 1.1 ϱ. The diagram further confirms that ϱ_{eff} is of the same order as s.
Rearranging Eq. 21, it can be derived that J_{Ic} values can be computed by determining the applied J-integral values at fracture initiation in notched specimens with $\varrho \geq \varrho_{eff}$ and calculating s by metallographic observations.
Table 1 reports experimental and calculated values of J_{Ic} for the C-Mn steels of Figs. 3 and 4. In the case of the steels tested by Chipperfield and Knott computed data have been obtained converting the δ_A/ϱ values, determined averaging their results, into J_A/ϱ values by the usual relationship, $J_A = 2\sigma_y\delta_A$. Results listed in Table 1 clearly indicate the close agreement between the values of fracture toughness calculated by the use of Eq. 21 and those measured on precracked samples. Only in one case (steel D) is the difference rather high, which might be abscribed to the data from which δ_A/ϱ was calculated. It is interesting to note that, in the case of steel T, the model and the relationships based on it yield satisfactory results with specimens differently oriented in respect to the rolling direction.
For the sake of comparison with equations 2 to 16, previously listed Eq. 19 can be converted to yield K_{Ic} by the usual relationship, $K_{Ic}^2 = E\,J_{Ic}/(1-\nu^2)$, to obtain,

$$K_{Ic} = \left\{ \frac{\sigma_y^{(1-N)}}{(1-\nu^2)} \; \frac{\varepsilon_{max,f}^{*\,(1+N)} E^{(1+N)}}{F(\Gamma(N))} \right\}^{1/2} s^{1/2} \qquad (22)$$

Eq. 22 employs all the five mechanical and microstructural quantities that enter with various arrangements in the previously examined equations. Although only one microstructural parameter, s, is directly indicated, the strong inverse dependance of $\varepsilon^*_{max,f}$ on v is evident from data reported about steels 1, 2, and 3. Fractographs reported in Fig. 5 clearly depict the strain localization promoted in steel 3 by the large inclusion fraction. In fact, fracture surfaces between long furrows formed around major inclusions are decidedly flatter in this steel than in the other two where, instead, coalescence between first voids occurs mainly due to continuous plastic flow (see also Fig. 6). Therefore it can be stated that K_{Ic} and J_{Ic} values are controlled both by the spacing between large inclusions and by the total second-phase volume fraction, whereas K_A and J_A values for blunt notch specimens depend mainly on v.

Fig. 6 - Detail of surface of steel 2 in the region of ductile fracture nucleation from a sharp crack.

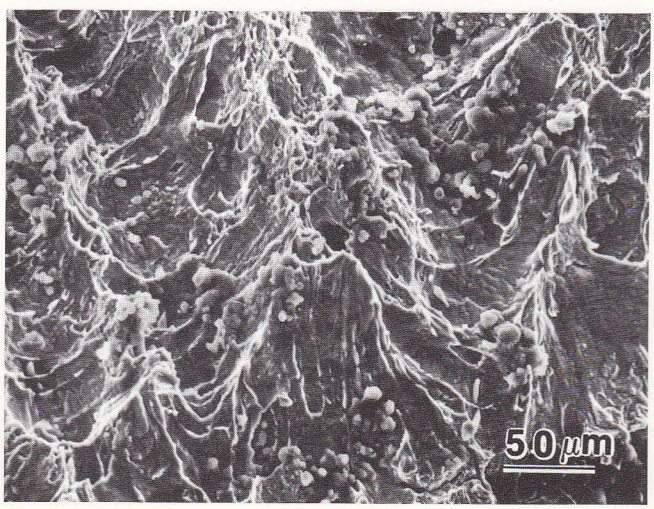

Conclusions

A new model for fully ductile fracture nucleation ahead of sharp cracks has been derived on the basis of experimental results on a number of low carbon, medium manganese steels. The model hypothesizes that crack tips blunt, up to achieving a finite root radius, ϱ_{eff}, which is of the same order of magnitude as the spacing between major non metallic inclusions, *s*. Then a fracture nucleates ahead of the blunted tip when the maximum strain at the root of the notch generated in the above way reaches a limiting value, $\varepsilon_{max,f}$, which is inversely proportional to the inclusion volume fraction. A procedure to calculate $\varepsilon^{*}_{max,f}$ values from the applied J-integral value at fracture initiation in a blunt notch specimen with notch-end radius greater than *s* has been described, and applied to compare calculated J_{Ic} values with experimental ones.

The model and the relationships based on it have been seen to work with very good approximation in the case of steels with a ferritic matrix. Experiments to prove its validity in the case of different metal alloys will be performed in the near future.

TABLE 1 - Comparison of experimental and calculated values of the fracture toughness for a number of C-Mn steels

Steel	Ref.	C %	Mn %	S %	J_A/ϱ (MN/m^2)	δ_A/ϱ	*s* (μm)	J_{Ic}(calc.) (MN/m)	J_{Ic}(exp.) (MN/m)
1	32	0.17	1.33	0.007	2083		110	0.229	0.194
2	32	0.17	1.33	0.017	1603		102	0.163	0.145
3	32	0.17	1.33	0.033	667		106	0.070	0.065
A	15,17	0.12	0.90	0.24		0.891	42	0.020	0.020
A' (o)	17	0.12	0.90	0.24		0.687	32	0.012	0.011
B (oo)	17	0.17	1.95	0.26		0.245	180	0.028	0.029
C	17	0.17	2.09	0.006		1.96	95	0.172	0.148
D	17	0.18	1.29	0.005		4.07	88	0.262	0.154
T (T-S)	17	0.18	1.42	0.035		1.59	65	0.067	0.064
T (L-S)						2.29	87	0.128	0.119
T (T-L)						0.60	131	0.051	0.041

(o) Same as steel A, but roll-bonded.
(oo) Inclusions were clustered, *s* is the mean spacing between clusters.

REFERENCES

*(1) Rice, J.R., and M.A. Johnson. The role of large crack tip geometry changes in plane strain fracture. In M.F. Kanninen, W.F. Adler, A.R. Rosenfield, R.I. Jaffee (Eds,), **Inelastic Behaviour of Solids**. Mc Graw. Hill, New York, N.Y. 1970, pp. 641-672.*

*(2) Ritchie, R.O., and R.M. Horn. Further considerations on the inconsistency in toughness evaluation of AISI 4340 steel austenitized at increasing temperatures. **Met. Trans. A, 9A** (1978), 331-341.*

*(3) Krafft, J.M. Correlation of plane strain toughness with strain hardening characteristics of a low, medium and a high strength steel. **Appl. Mat. Res., 3** (1964), 88-101.*

*(4) Birkle, A.J., R.P. Wei, and G.E. Pellissier. Analysis of plane-strain fracture in a series of 0.45C-Ni-Cr-Mo steels with different sulfur content. **Trans. ASM, 59** (1966), 1981-990.*

*(5) Beachem, C.D., and G.R. Yoder. Elastic-plastic fracture by homogeneous microvoid coalescence tearing along alternating shear planes. **Met. Trans., 4** (1973), 1145-1153.*

*(6) Yoder, G.R. Fractographic lines in maraging steel-A link to fracture toughness. **Met. Trans., 4** (1973), 1851-1859.*

*(7) Clausing, D.P. Effect of plastic strain state on ductility and toughness. **Int. J. Fract. Mech., 6** (1969), 71-85.*

(8) Krafft, J.M. Role of local dissolution in corrosion-assisted cracking of titanium alloys. Presented at the Nat. Symp. on Fract. Mech., Lehigh Univ. Betlehem, Pa., USA, (1967).

*(9) Hahn, G.T., and A.R. Rosenfield. Sources of fracture toughness: the relation between K_{Ic} and the ordinary tensile properties of metals. In **Application Related Phenomena in Titanium Alloys, ASTM STP 432**, American Society for Testing and Materials, 1968, pp 5-32.*

*(10) Slatcher, S., and J.F. Knott. The ductile fracture of high strength steels. In D. Francois (Ed.), **Advances in Fracture Mechanics**, Pergamon Press, Oxford, vol. I, 1981, pp. 201-207.*

*(11) Chen, C.Q., and J.F. Knott. Effect of dispersoid particles on toughness of high strength aluminum alloys. **Met. Sc., 15** (1981), 357-364.*

*(12) Hahn, G.T., and A.R. Rosenfield. Metallurgical factors affecting fracture toughness of aluminum alloys. **Met. Trans. A, 6A** (1975), 653-668.*

(13) Broek, D. The role of inclusions in ductile fracture and fracture

toughness. **Engnr. Fract. Mech., 5** (1973), 55-66.

(14) Barsom, J.M., and J.V. Pellegrino. Relationship between K_{Ic} and plane strain tensile ductility and microscopic mode of fracture. **Engnr. Fract. Mech., 5** (1973), 209-221.

(15) Smith, R.F., and J.F. Knott. Crack opening displacement and fibrous fracture in mild steel. In **Practical applications of fracture mechanics to pressure vessel technology**. I. Mech. Eng., London, 1971, pp. 65-75.

(16) Griffiths, J.R., and D.R.J. Owen. An elastic-plastic analysis for a notched bar in plane strain bending. **J. Mech. Phys. Solids, 19** (1971), 419-431.

(17) Chipperfield, G.C., and J.F. Knott. Microstructure and toughness of structural steels. **Metals Techn., 2** (1975), 45-51.

(18) Schwalbe, K.H. Crack propagation in AlZnMgCu 0.5 during static loading. **Eng. Fract. Mech., 6** (1974), 415-434.

(19) Schwalbe, K.H. On the influence of microstructure on crack propagation mechanisms and fracture toughness of metallic materials. **Eng. Fract. Mech., 9** (1977), 795-832.

(20) Rice, J.R. Stresses due to a sharp notch in a work-hardening elasticplastic material loaded by longitudinal shear. **J. Appl. Mech., Trans. ASME E, 34** (1967), 267-298.

(21) Osborne, D.E., and J.D. Embury. The influence of warm rolling oh the fracture toughness of bainitic steels. **Met. Trans., 4** (1973), 2051-2061.

(22) Rice, J.R., and G.F. Rosengren. Plane strain deformation near a crack tip in a power-law hardening material. **J. Mech. Phys. Solids, 16** (1968), 1-12.

(23) Pandey, R.K., and S. Banerjee. Strain induced fracture in low strength steels. **Eng. Fract. Mech., 10** (1978), 817-829.

(24) Ritchie, R.O., W.L. Server, and R.A. Wullaert. Critical fracture stress and fracture strain models for the prediction of lower and upper shelf toughness in nuclear pressure vessel steels. **Met. Trans. A, 10A** (1979), 1557-1570.

(25) Mc Meeking, R.M. Finite deformation analysis of crack tip opening in elastic-plastic materials and implications for fracture. **J. Mech. Phys. Sol., 25** (1977), 357-381.

(26) Mackenzie, A.C., J.W. Hancock, and D.K. Brown. On the influence of state of stress on ductile failure initiation in high strength steels. **Eng. Fract. Mech., 9** (1977), 167-188.

(27) Gensamer, M., E.B. Pearsal, W.S. Pellini, J.R. Low, Jr. The tensile properties of pearlite, bainite and spheroidite. **Trans. ASM, 30** (1942), 983-1020.

(28) Gensamer M. Strength and ductility. **Trans. ASM, 36** (1946), 30-60.

(29) Pickering, F.B. The effect of composition and microstructure on ductility and toughness. In **Toward improved ductility and toughness**. I.S.I. Japan, Japan Inst. Met., 1971, pp. 9-31.

(30) Spretnak, J.W., and D. Firrao. The role of plastic instability in ductile fracture. **Metall. Ital., 72** (1980), 525-534.

(31) Lereim, J., and J.D. Embury. Some aspects of the process zone associated with the fracture of notched bars. In **What does the Charpy test really tell us?** ASM, Metals Park, Ohio, 1978, pp. 33-53.

(32) Roberti, R., G. Silva, D. Firrao, and B. De Benedetti. Influence of notch root radius on ductile rupture fracture toughness evaluation with Charpy-V type specimens. **Int. J. Fatigue, 3** (1981), 133-141.

(33) Firrao, D., G. Silva, R. Roberti, B. De Benedetti, and J.A. Begley. The blunt notch fracture toughness of as-quenched AISI 4340 steel. **VDI-Z Fortschr.-Berichte**, series 18, no. 6, 1979, 157-169.

(34) Firrao, D., J.A. Begley, R. Roberti, G. Silva, and B. De Benedetti. The influence of notch root radius and austenitizing temperature on fracture appearance of as-quenched Charpy-V type AISI 4340 steel specimens. **TMS-AIME Paper no. A80-61**, 1980, 1-21. **Met. Trans. A, 13A** (1982), 1003-1013.

(35) Firrao, D., R. Roberti, and G. Silva. The role of microstructure and notch root radius on the fracture toughness of a martensite structure steel. In K.L. Maurer, F.E. Matzer (Eds.), **Fracture and the role of microstructure**, Emas, Warley, vol. II, 1982, pp. 727-735.

(36) Begley, J.A., W.A. Logsdon, and J.D. Landes. Ductile rupture blunt notch fracture criterion. In J.B. Wheeler (Ed.), **Flaw Growth and Fracture, ASTM STP 631**. American Society for Testing and Materials, Philadelphia, 1977, pp. 112-120.

(37) Rice, J.R. A path independent integral and the approximate analysis of strain concentration by notches and cracks. **J. Appl. Mech., Trans. ASME E, 35** (1968), 379-386.

(38) Firrao, D., and R. Roberti. A model for plane strain ductile fracture toughness. In R.C. Gifkins (Ed.), **Strength of metals and alloys** (1982), Pergamon Press, Oxford, 1982, pp. 947-952.

(39) Firrao, D., and R. Roberti. Sui parametri microstrutturali che controllano la tenacità alla frattura degli acciai. **Met. Ital., 75** (1983), in press.